

MIA RADONJIĆ<sup>1,2,\*</sup>  
JELENA PETROVIĆ<sup>1,2,\*</sup>  
MILENA MILIVOJEVIĆ<sup>3</sup>  
MILENA STEVANOVIĆ<sup>3,4,5</sup>  
JASMINA STOJKOVSKA<sup>1,2</sup>  
BOJANA OBRADOVIĆ<sup>1</sup>

<sup>1</sup> University of Belgrade, Faculty  
of Technology and Metallurgy,  
Belgrade, Serbia

<sup>2</sup> Innovation Center of the Faculty of  
Technology and Metallurgy, Serbia

<sup>3</sup> University of Belgrade, Institute  
of Molecular Genetics and Genetic  
Engineering, Belgrade, Serbia

<sup>4</sup> University of Belgrade, Faculty of  
Biology, Belgrade, Serbia

<sup>5</sup> Serbian Academy of Sciences and  
Arts, Belgrade, Serbia

\* Authors contributed equally to this  
work

SCIENTIFIC PAPER

UDC 66.02:616-006.6:51

## CHEMICAL ENGINEERING METHODS IN ANALYSES OF 3D CANCER CELL CULTURES: HYDRODYNAMIC AND MASS TRANSPORT CONSIDERATIONS

### Article Highlights

- Chemical engineering methods provide explanations for experimental findings in 3D cell cultures
- Shear stress levels of  $\sim 70$  mPa may induce cell death in 3D glioma cell cultures
- Perfusion enhanced proliferation of C6 glioma cells in microfibers as compared to static controls
- Perfusion is necessary for the mass transport of molecules with low diffusivities of  $\sim 10^{-19}$  m<sup>2</sup> s<sup>-1</sup>

### Abstract

*A multidisciplinary approach based on experiments and mathematical modeling was used in biomimetic system development for three-dimensional (3D) cultures of cancer cells. Specifically, two cancer cell lines, human embryonic teratocarcinoma NT2/D1 and rat glioma C6, were immobilized in alginate microbeads and microfibers, respectively, and cultured under static and flow conditions in perfusion bioreactors. At the same time, chemical engineering methods were applied to explain the obtained results. The superficial medium velocity of  $80 \mu\text{m s}^{-1}$  induced lower viability of NT2/D1 cells in superficial microbead zones, implying adverse effects of fluid shear stresses estimated as  $\sim 67$  mPa. On the contrary, similar velocity ( $100 \mu\text{m s}^{-1}$ ) enhanced the proliferation of C6 glioma cells within microfibers compared to static controls. An additional study of silver release from nanocomposite Ag/honey/alginate microfibers under perfusion indicated that the medium partially flows through the hydrogel (interstitial velocity of  $\sim 10$  nm s<sup>-1</sup>). Thus, a diffusion-advection-reaction model described the mass transport to immobilized cells within microfibers. Substances with diffusion coefficients of  $\sim 10^{-9}$ - $10^{-11}$  m<sup>2</sup> s<sup>-1</sup> are sufficiently supplied by diffusion only, while those with significantly lower diffusivities ( $\sim 10^{-19}$  m<sup>2</sup> s<sup>-1</sup>) require additional convective transport. The present study demonstrates the selection and contribution of chemical engineering methods in tumor model system development.*

*Keywords: tumor engineering, alginate hydrogel, perfusion bioreactor, mathematical modeling, glioma C6 cell line, embryonic teratocarcinoma NT2/D1 cell line.*

Cancer is the second leading cause of death

worldwide; searching for its cure is one of the most important challenges in the 21<sup>st</sup> century (over 19 million new cases in 2020 [1]). One of the underlying problems is the complex and slow development of new anticancer drugs, which traditionally rely on two-dimensional (2D) cell cultures followed by *in vivo* studies on animals. However, 2D cultures have many limitations, including different cell morphology, polarity, duplication time, and absence of interactions with extracellular components [2]. Thus, 2D cell cultures fail

Correspondence: B. Obradović, University of Belgrade, Faculty of Technology and Metallurgy, Karnegijeva 4, 11000 Belgrade, Serbia.

E-mail: [bojana@tmf.bg.ac.rs](mailto:bojana@tmf.bg.ac.rs)

Paper received: 7 June, 2021

Paper revised: 7 September, 2021

Paper accepted: 17 September, 2021

<https://doi.org/10.2298/CICEQ210607033R>

to adequately simulate the complexity of the tumor microenvironment *in vivo*, which involves three-dimensional (3D) structures and extracellular matrix (ECM), allowing cell-cell and cell-ECM interactions that control tumor growth and progression [3]. These substantial interactions are absent in 2D cell cultures, frequently leading to inconsistencies in the efficacies of anticancer drugs observed *in vitro* compared to the results obtained in clinical trials [4]. On the other hand, animal models in preclinical trials often produce misleading results due to native interspecies differences [5]. Hence, there is an emerging necessity for developing more relevant 3D *in vitro* tumor models, which would mimic the tumor microenvironment and provide a more accurate translation of the results to *in vivo* settings. In addition, reliable 3D *in vitro* tumor models could significantly reduce animal testing and serve as consistent systems for investigations and development of novel anticancer drugs.

However, transitioning from 2D to 3D cell culture models goes hand in hand with the increase in system complexity, which requires multidisciplinary approaches. Applying chemical engineering principles in developing *in vitro* tumor model systems has already shown undeniable potential. Mathematical modeling can analyze and better understand tumor behavior in growth, progression, and invasion [6-8]. Additionally, model-based predictions can be used to evaluate the effects of anticancer drugs [7-9]. One of the approaches in tumor engineering relies on the tissue engineering strategy based on the integrated use of scaffolds for cell attachment and support and biomimetic bioreactors providing efficient mass transport and adequate physical signals [10]. In this approach, chemical engineering principles arise as a powerful tool for insight into the underlying phenomena and overcoming experimental trial-and-error methodology in system optimization [11-14].

This work shows the potential of applying chemical engineering principles to analyze experimental results to gain more accurate insights into the mechanisms occurring in our 3D *in vitro* systems for cancer cell culture. Specifically, two types of cancer cells were cultured in a biomimetic 3D system consisting of alginate hydrogels as cell carriers and perfusion bioreactor. Alginate was chosen due to its biocompatibility, immunogenicity, and non-toxicity [15]. In the presence of multivalent cations, *e.g.*,  $\text{Ca}^{2+}$ , alginate solutions undergo rapid and mild gelation forming hydrogels that can be produced in different shapes (beads, fibers, and films) and sizes (*e.g.* [16,17]). Due to its structural similarity to native ECMs of soft tissues, alginate hydrogels have been widely

used in wound dressings, controlled drug delivery systems, *in vitro* cell cultures, and tissue engineering [15]. In tumor engineering, alginate-based scaffolds in different forms support cell viability and proliferation *in vitro* [18] and cell conversion to more malignant *in vivo*-like phenotypes compared to 2D cultures [19-21]. *In vivo*, alginate-based scaffolds supported tumor growth and blood vessel recruitment [19,20]. Also, this type of cell carrier induced the formation of multicellular tumor spheroids *in vitro* [22-26] that retained high cell viability [22], increased invasion and metastatic potential [23], and higher expression of tumor angiogenesis biomarker [25] than cells in 2D cultures. Furthermore, alginate-based 3D tumor models showed increased resistance to anticancer drugs than monolayer cultures indicating a closer resemblance to the natural tumor environment [20,23,25].

Contrary to the cells grown in the monolayer having unlimited access to the ingredients of the medium, the supply of oxygen and nutrients to the cells in 3D tumor models may become critically limited. Thus, perfusion bioreactors have been occasionally applied to improve mass transport to and from cultivated cells by laminar flow of the medium at physiological velocities directly through a scaffold with cells. The increased cell viability and proliferation under 3D perfusion conditions as opposed to static cultures were reported for several cancer cell lines and cancer spheroid models [27-29]. Furthermore, 3D perfusion systems supported structural maintenance of cancer tissue *in vitro* [30-32]. Several studies reported significantly altered biological responses to anticancer therapies of tumor cultures grown under perfusion conditions compared to standard 2D monolayer cultures, thus suggesting 3D perfusion systems as more relevant *in vitro* models for testing cancer sensitivity to drugs [28,29,32-34]. Still, medium flow in perfusion systems induces hydrodynamic shear stresses on exposed cells and scaffold surfaces, possibly causing negative effects. For example, fluid flow in collagen gels loaded with glioma cells induced compaction of the gels while suppressing the migratory activity of U87 and CNS-1 glioma cell lines proportionally to the shear stress level and duration of shear stress exposure [35]. Shear stresses of magnitudes above 1 Pa induced cell death in monolayers of differentiated human neuroblastoma SH-SY5Y cells characterized by DNA fragmentation [36] and a monolayer of a human hepatocellular liver carcinoma HepG2 cell line [37]. In a study of circulating metastatic breast cancer cells (MDA-MB-231), shear stresses of 0.5 and 2 Pa decreased viability of individual cells and induced disaggregation of cell clusters [38]. Interestingly, based on these results and findings published in the literature, the authors concluded that

shear stress levels inducing death of circulating tumor cells might, at the same time, increase the aggressiveness of the surviving cells by fostering cell capabilities for migration and adhesion to metastatic sites [38]. Thus, in 3D culture systems, the flow rate has to be optimized to provide efficient mass transport at acceptable shear stress levels, which may vary depending on the cell type. Therefore, chemical engineering analysis of hydrodynamic and mass transport conditions is the subject matter, which can provide directions to optimize system parameters (*e.g.*, flow rate, scaffold size, and geometry). In addition, these analyses offer possibilities to identify critical factors (*e.g.*, shear stress, limiting nutrient or active substance) affecting the cells in a 3D culture to correlate the cell microenvironment with the observed effects (*e.g.*, cell viability, metabolic activity, proliferation rate).

In this work, we conducted two independent experiments using two forms of alginate hydrogels and a perfusion bioreactor and applied chemical engineering principles to analyze the obtained results. In addition, a separate experimental study with nanocomposite Ag/honey/alginate microfibers was conducted to determine mass transport mechanisms under perfusion. Then, hydrodynamic shear stresses were determined, and mass transport modeling was applied to elucidate the experimentally observed effects of cultivation conditions on the cultured cancer cells.

## MATERIALS AND METHODS

### Materials

Low viscosity sodium alginate (A3249) was supplied from AppliChem (Germany). Two batches of acacia honey from different suppliers (Azad.o.o., S. Ledinci, Serbia and Venenum Apis, Smedervska Palanka, Serbia) were used for the synthesis of silver nanoparticles (AgNPs). Silver nitrate (AgNO<sub>3</sub>) was purchased from Pliva (Zagreb, Croatia). Dulbecco's modified Eagle's medium (DMEM, 4.5 g dm<sup>-3</sup> glucose), fetal bovine serum (FBS), and Penicillin-Streptomycin-Amphotericin B solution (Pen-Strep-Ampho. B) were supplied from Biological Industries (Israel). Calcium chloride dihydrate (CaCl<sub>2</sub>·2H<sub>2</sub>O) was provided by Acros Organics (USA). Phosphate-buffered saline (PBS), calcium nitrate tetrahydrate (Ca(NO<sub>3</sub>)<sub>2</sub>·4H<sub>2</sub>O), sodium citrate dihydrate (Na<sub>3</sub>C<sub>6</sub>H<sub>5</sub>O<sub>7</sub>·2H<sub>2</sub>O), sodium hydroxide (NaOH), L-glutamic acid, Trypsin/EDTA, Trypan Blue solution, and methylthiazolyldiphenyl-tetrazolium bromide (MTT) were all purchased from Sigma-Aldrich (USA). LIVE/DEAD™ Cell Imaging Kit was supplied from Thermo Fisher Scientific (Waltham,

MA, USA).

### Cell lines

The rat glioma cell line C6 (ATCC® CCL-107™) and the human embryonic teratocarcinoma cell line NTERA-2 cl.D1 (also known as NT2/D1; ATCC® CRL-1973™; a kind gift from Prof. Peter W. Andrews, University of Sheffield, UK) were maintained in the culture medium (DMEM supplemented with 10% FBS, 2 mM L-glutamine, and 1% Pen-Strep-Ampho.B). The cultures were incubated at 37 °C in a fully humidified atmosphere with 5% CO<sub>2</sub> (C6 cells) or 10% CO<sub>2</sub> (NT2/D1 cells).

When the confluence of about 90% was reached, cells were detached using 0.25% Trypsin /1mM EDTA. In brief, cells in 10 cm Petri dishes were washed with 5 cm<sup>3</sup> 1xPBS, treated with 1 cm<sup>3</sup> Trypsin /EDTA for 5 min at 37 °C, after which Trypsin /EDTA was neutralized with DMEM.

### Cell immobilization in alginate hydrogels

Two different independent experiments were conducted. In Experiment 1, NT2/D1 cells were immobilized in alginate microbeads, while in Experiment 2, C6 cells were immobilized in alginate microfibers. Alginate microbeads and microfibers were produced as follows: sodium alginate powder was dissolved in distilled water at 2% w/w and 3.5% w/w, respectively, and the obtained solutions were sterilized by boiling for 30 min. Before immobilization, cells were detached using Trypsin/EDTA (as described above) and counted using a hemocytometer.

#### *Immobilization of NT2/D1 cells in alginate microbeads (Experiment 1)*

A suspension of NT2/D1 cells was mixed with 2% w/w sodium alginate solution to obtain final concentrations of 1.3% w/w alginate and 1×10<sup>6</sup> cells cm<sup>-3</sup>. Alginate microbeads with the immobilized NT2/D1 cells were produced by electrostatic droplet generation (4.3 kV electrostatic potential, 2.5 cm electrode distance), using a blunt edge needle (28 G, Small Parts Inc., USA), a flow rate of 25.2 cm<sup>3</sup> h<sup>-1</sup>, and a gelling solution containing Ca<sup>2+</sup> (0.18 M CaCl<sub>2</sub>·2H<sub>2</sub>O), as described previously [39]. The obtained microbeads were left in the gelling solution for 15 min to complete gelling and subsequently washed with the culture medium. The microbeads were further placed into the fresh medium and cultivated for the next 24 h under static conditions in a humidified incubator at 10% CO<sub>2</sub> and 37 °C.

#### *Immobilization of rat glioma C6 cells in alginate microfibers (Experiment 2)*

A suspension of rat glioma C6 cells was mixed

with 3.5 % w/w sodium alginate solution to obtain final concentrations of 2.8 % w/w alginate and  $8 \times 10^6$  cells  $\text{cm}^{-3}$ . Alginate microfibers with immobilized C6 cells were produced by manual extrusion of the obtained suspension through a blunt edge stainless steel needle (25 G, Small Parts Inc., USA) immersed in the gelling solution containing  $\text{Ca}^{2+}$  (0.18 M  $\text{Ca}(\text{NO}_3)_2 \cdot 4\text{H}_2\text{O}$ ). The resulting microfibers were left in the gelling solution for 15 min to complete gelling. After washing with the culture medium, the microfibers were placed into the fresh medium and cultivated for the next 8 days under static conditions in a humidified incubator at 5%  $\text{CO}_2$  and 37 °C. Specifically, 0.5 g of microfibers were maintained in 15  $\text{cm}^3$  medium, while 40% of the medium was replaced every 4<sup>th</sup> day.

### Cultivation of immobilized cells in perfusion bioreactors

#### *Bioreactor cultivation of microbeads with immobilized NT2/D1 cells*

A perfusion bioreactor system used to cultivate alginate microbeads with immobilized NT2/D1 cells consisted of a chamber, two 3-way stopcocks, a medium reservoir, and a silicone tubing loop as described previously [40]. In the present experimental setup, 0.5 g of wet microbeads with immobilized NT2/D1 cells, 24 h after immobilization, was placed in the bioreactor chamber (0.8 cm inner diameter, 1.5 cm height) formed by a piece of silicone tubing, and the system was filled with 11  $\text{cm}^3$  of the culture medium. Three perfusion systems were set up and placed in the incubator at 37 °C and fully humidified atmosphere with 10%  $\text{CO}_2$ . The flow rate of 0.25  $\text{cm}^3 \text{min}^{-1}$ , which corresponded to the superficial velocity of 80  $\mu\text{m s}^{-1}$ , was provided by a multichannel peristaltic pump (Masterflex, Cole-Parmer, IL, USA) placed outside the incubator. The static culture comprising 3 Petri dishes with 0.5 g of wet microbeads with immobilized NT2/D1 cells in 11  $\text{cm}^3$  of the culture medium, each, served as a control. The experiment lasted for 10 days, and 40% of the culture medium was changed twice a week.

#### *Bioreactor cultivation of microfibers with immobilized C6 cells*

The single-use perfusion bioreactor system “3D Perfuse” (Innovation Center of the Faculty of Technology and Metallurgy, Belgrade, Serbia) was used to cultivate alginate microfibers with immobilized rat glioma C6 cells. The system consisted of a chamber, two 3-way stopcocks, a medium reservoir, and a silicone tubing loop serving for gas exchange [41]. In the present experimental setup, 0.5 g of wet microfibers with the immobilized rat glioma C6 cells, cultured statically for 8 days, was placed in the

bioreactor chamber (0.8 cm inner diameter, 4 cm height) formed by a piece of silicone tubing and the system was filled with 15  $\text{cm}^3$  of the culture medium. Two perfusion systems were set up and placed in the incubator at 37 °C and fully humidified atmosphere with 5%  $\text{CO}_2$ . The flow rate of 0.30  $\text{cm}^3 \text{min}^{-1}$ , which corresponded to the superficial velocity of 100  $\mu\text{m s}^{-1}$ , was provided by a multichannel peristaltic pump (Masterflex, Cole-Parmer, IL, USA) placed outside the incubator. The static culture comprising 2 Petri dishes with 0.5 g of wet microfibers with immobilized C6 cells and 15  $\text{cm}^3$  of the culture medium served as a control. On the 4<sup>th</sup> day of the experiment, 40% of the culture medium was changed, while the experiment lasted for 5 days.

### Production of Ag/honey/alginate microfibers and silver release studies

AgNPs were obtained by chemical reduction of silver ions in aqueous solutions of two batches of honey, as described previously [42]. In brief, honey was dissolved in distilled water at the final concentration of 50% w/w. Then, silver nitrate was added to the solution to achieve the final concentration of silver of 3.9 mM. Next, 1 M NaOH was added dropwise to initiate the reduction of  $\text{Ag}^+$  ions and to increase the pH value to 9. After achieving the desired pH value, the solution was left in the dark for 4 days and at room temperature. Next, the solution was mixed with the aqueous solution of sodium alginate to achieve final concentrations of 2.8% w/w alginate, 30% w/w honey, and 2.34 mM silver. The composite microfibers were produced by manual extrusion of the obtained solution into the gelling solution, containing  $\text{Ca}^{2+}$  (0.73 M  $\text{Ca}(\text{NO}_3)_2 \cdot 4\text{H}_2\text{O}$ ), through a blunt edge stainless steel needle (22 G, Small Parts Inc., USA) and were left in the gelling solution for 30 min to complete gelling. Finally, composite silver/honey/alginate microfibers were placed in distilled water and kept in the dark at 4 °C.

Silver release studies were performed in the same “3D Perfuse” perfusion system comprising 0.5 g of nanocomposite microfibers and 15  $\text{cm}^3$  of the culture medium in each recirculation loop. Three bioreactor systems for each time point were kept in the incubator at 37 °C and fully humidified atmosphere with 5%  $\text{CO}_2$  and continuously perfused at the flow rate of 0.25  $\text{cm}^3 \text{min}^{-1}$  corresponding to the superficial velocity of 80  $\mu\text{m s}^{-1}$ . The experiments lasted for 1, 2, 5, and 7 days, at which time points the medium was analyzed for silver concentration.

### Analytical methods

#### *Optical microscopy*

The average microbead diameter was determined using a DM IL LED Inverted Microscope (Leica Micro-

systems, Germany) from measurements of at least 20 microbeads using the Leica Application Suite V4.3.0 software. Images of LIVE/DEAD assays were taken by an Olympus BX51 Fluorescence Microscope (Olympus, Japan). An optical microscope Olympus Vanox (Olympus, Japan), was used for cell counting. The optical microscope Motic BA210 (Motic, China) connected to software for image analysis (Motic Images Plus 2.0) was used to measure microfiber diameters. The average microfiber diameter was determined from at least 10 measurements.

#### *Determination of cell density and viability*

A portion of microbeads/microfibers (0.2 - 0.3 g) was dissolved in 2% w/v sodium citrate solution at the hydrogel to a solution mass ratio of 1:5 to determine the number of viable cells in alginate hydrogels. Then, 100  $\mu\text{l}$  of the obtained cell suspension was mixed with 100  $\mu\text{l}$  of Trypan Blue solution, and the cells were counted after 5 min using a hemocytometer and an optical microscope. Finally, cell viability was calculated using the ratio of the number of unstained (viable) cells and the total cell count.

#### *Live/Dead Staining*

Cell viability in Experiment 1 was assessed by using a LIVE/DEAD™ Cell Imaging Kit (R37601, Thermo Fisher Scientific, USA) and staining according to the manufacturer's protocol. The kit discriminates live cells (green fluorescence) from dead cells (red fluorescence). Cells were visualized using an Olympus BX51 fluorescence microscope, a FITC filter for green fluorescence, and a Texas Red filter for a red fluorescence and analyzed using Cytovision 3.1 software (Applied Imaging Corporation, USA). All images were captured by using a 20x objective. In brief, 2-3 microbeads with immobilized NT2/D1 cells were transferred into a tube with 50  $\mu\text{l}$  of the culture medium and mixed with the equal volume of the Live Green/Dead Red solution. The samples were incubated for 20 min at room temperature and then transferred to microscope slides and immediately imaged.

#### *MTT assay*

The MTT assay was used at the end of Experiment 2 to assess cell viability within the microfibers. In brief, the MTT reagent was dissolved in PBS and then diluted to 0.5 mg  $\text{cm}^{-3}$  with the culture medium. Next, 0.1 g of microfibers was incubated with 1  $\text{cm}^3$  of the MTT solution in a 24 well plate, and the images of microfibers were taken after 15 h using an optical microscope.

#### *UV-vis spectroscopy*

UV-visible spectroscopy (model UV-3100, Mapada, China) was used to investigate the presence of AgNPs in the colloid solution and in the obtained nanocomposite microfibers as described previously [42].

#### *Silver concentration*

The initial silver concentration in microfibers was determined upon microfiber (0.1 g) dissolution in 2% w/v sodium citrate solution (3  $\text{cm}^3$ ), followed by the addition of 10  $\text{cm}^3$  of  $\text{NH}_4\text{OH}$  solution (25%). The culture medium samples were mixed with 25%  $\text{NH}_4\text{OH}$  in the volume ratio of 2:1 to oxidize potentially released AgNPs and dissolve precipitated AgCl. At the same time, perfusion loops and Petri dishes were rinsed with the same alkaline solution. Finally, silver concentration in all obtained solution samples was determined by atomic absorption spectroscopy (AAS) using an Agilent Technologies 240FS AA spectrophotometer (Agilent Technologies, USA).

## RESULTS AND DISCUSSION

### **Cultivation of alginate microbeads with immobilized NT2/D1 cells**

Microbeads with immobilized NT2/D1 cells were obtained by electrostatic extrusion of the cell suspension in sodium alginate ( $1 \times 10^6$  cells  $\text{cm}^{-3}$  and 1.3% w/w sodium alginate). The average diameter of the resulting microbeads was  $310 \pm 20$   $\mu\text{m}$ , while the immobilized cell concentration was  $2.3 \times 10^6$  cells  $\text{cm}^{-3}$ . The increase in the cell concentration after immobilization could be explained by the syneresis of alginate gel during gelation, as reported previously for the production of nanocomposite Ag/alginate microbeads [43,44].

NT2/D1 cells immobilized in alginate microbeads were cultivated under continuous perfusion at the flow rate of 0.25  $\text{cm}^3 \text{min}^{-1}$  (superficial velocity of 80  $\mu\text{m s}^{-1}$ ) for 10 days. At the end of the experiment, the microbead diameter slightly increased in the bioreactor ( $360 \pm 30$   $\mu\text{m}$ ) and the static culture ( $370 \pm 30$   $\mu\text{m}$ ). However, it was impossible to accurately determine the cell concentration within microbeads due to the adverse effects of the alginate dissolution process by the citrate solution. Yet, to get an insight into the cell viability, the microbeads were stained with the LIVE/DEAD Cell Imaging Kit, which revealed higher cell viability in the static culture (Fig. 1a) than the bioreactor culture (Fig. 1b). Furthermore, the immobilized cells were metabolically active in the core of microbeads in the bioreactor while inactive in the superficial microbead zone. These results indicate that mass transport in the

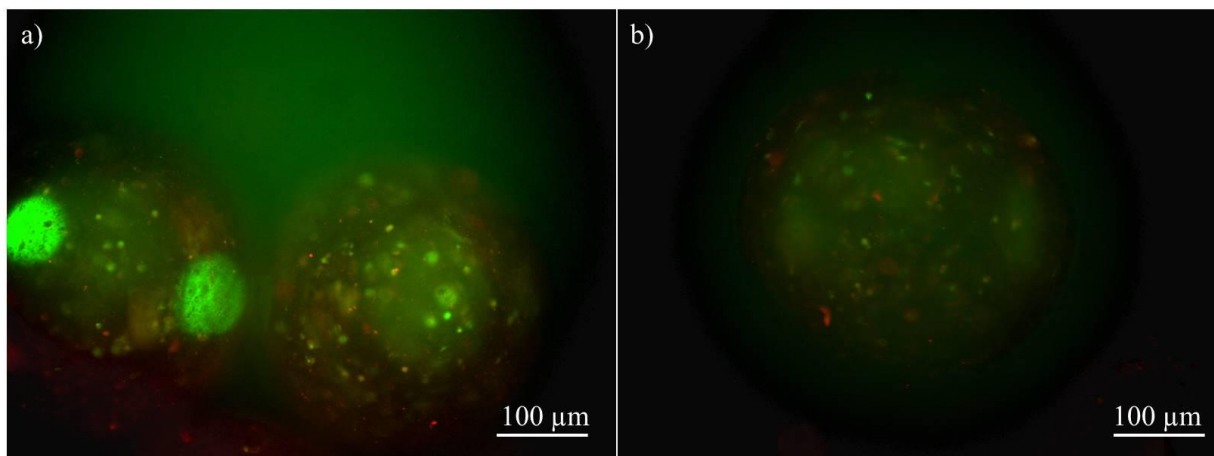


Figure 1. Fluorescence microscopy LIVE/DEAD Cell Imaging of NT2/D1 cells in microbeads after 10-day cultivation under a) static conditions; b) continuous perfusion in the perfusion bioreactor (scale bar: 100  $\mu\text{m}$ ); live cells (green), dead cells (red).

static culture and, therefore, in the bioreactor culture was sufficient to support cell viability. On the other hand, the adverse effects in the microbead superficial zones in the bioreactor culture could be thus attributed to shear stresses generated by the medium flow through the packed bed, which negatively influenced the cells.

#### Calculation of hydrodynamic shear stresses in the bioreactor with the packed bed of alginate microbeads

The well-known Carman - Kozeny equation was used to calculate the pressure drop per bed height ( $\Delta P/H$ ) to quantify the effects of shear stresses in the perfusion bioreactor. This equation was recommended for laminar flow in packed beds in a circular channel [45] and was applied for the packed bed of alginate microbeads as:

$$-\frac{\Delta P}{H} = 180 \frac{(1-\varepsilon)^2}{\varepsilon^3} \frac{\mu}{d_p^2} U \quad (1)$$

where  $\varepsilon$  is the packed bed porosity,  $\mu$  is the fluid viscosity,  $d_p$  is the particle diameter, and  $U$  is the superficial liquid velocity. The particle diameter value of 335  $\mu\text{m}$  was used, corresponding to the average microbead diameter in the bioreactor culture at the beginning end of the present experiment. The bed porosity was calculated as 0.27, considering the microbead mass (0.5 g) and the chamber volume. The viscosity of the cell medium was adopted as  $9.4 \times 10^{-4} \text{ Pa}\cdot\text{s}$  [46]. At the experimental superficial medium velocity of  $80 \mu\text{m s}^{-1}$ , the pressure drop was calculated as  $3266 \text{ Pa m}^{-1}$  by applying Eq. (1). This value was further used for calculation of the shear stress ( $\tau$ ) to which the microbeads were exposed as [45]:

$$\tau = \frac{\varepsilon}{S_v(1-\varepsilon)} \left( -\frac{\Delta P}{H} \right) \quad (2)$$

where  $S_v$  is the specific surface area of the particle. For the adopted microbead diameter,  $S_v$  was calculated as  $1.8 \times 10^4 \text{ m}^2 \text{ m}^{-3}$ , yielding the shear stress value of 67 mPa.

Cancer cells can be exposed to shear stresses generated by the blood flow, which affects circulating tumor cells, and the interstitial fluid flow in the ECM, influencing the cells of a growing tumor [47]. Qazi *et al.* [35] calculated the shear stress in brain tumors as 9 - 68 mPa based on the experimentally measured fluid velocities previously reported. Moreover, in the same work, it was shown that the shear stress of 55 mPa applied for 4 h practically diminished the migratory activity of the glioma cell line U87 and highly suppressed that of the CNS-1 glioma cell line. Still, it did not affect the U251 glioma cell line. At the same time, the adverse effects of the applied shear stress on the cell viability were not observed [35]. However, the calculated shear stress value in the present study is on the upper limit of the reported physiological range. Furthermore, it was constantly applied for 10 days, so it could be assumed that observed cell death in microbead superficial zones is caused by the applied shear stress.

#### Cultivation of alginate microfibers with immobilized rat glioma C6 cells

Microfibers ( $440 \pm 40 \mu\text{m}$  in diameter) with immobilized rat glioma C6 cells were obtained by manual extrusion of the cell suspension in sodium alginate. The cell concentration was  $2.5 \times 10^6 \text{ cells cm}^{-3}$  24 h after immobilization, significantly lower than the initial concentration in the suspension due to the cell loss in the foam formed during the mixing and extrusion

of the suspension. The obtained microfibers were then cultured in culture dishes under static conditions for 8 days, after which period the cell concentration was determined as  $1.5 \times 10^6$  cells  $\text{cm}^{-3}$ . The decrease in cell concentration might be caused by microfiber swelling to the average diameter of  $540 \pm 50$   $\mu\text{m}$  or might be the result of some adverse effects of cultivation conditions.

The microfibers were cultured in perfusion bioreactors for the next 5 days, parallel with static cultures that served as a control. The microfiber diameters did not further change significantly as compared to the starting value, being  $570 \pm 120$   $\mu\text{m}$  and  $520 \pm 100$   $\mu\text{m}$  under perfusion and static conditions, respectively. On the contrary, cell counting at the end of the experiment has shown that the applied flow rate of  $0.30$   $\text{cm}^3$   $\text{min}^{-1}$  (superficial velocity of  $100$   $\mu\text{m}$   $\text{s}^{-1}$ ) enhanced cell proliferation yielding the cell concentration of  $8.8 \times 10^6$  cells  $\text{cm}^{-3}$ . On the other hand, the cell concentration in microfibers cultivated under static conditions just slightly increased to  $1.7 \times 10^6$  cells  $\text{cm}^{-3}$  compared to the initial cell concentration (*i.e.*,  $1.5 \times 10^6$  cells  $\text{cm}^{-3}$ ). It should be noted that cell viability was  $\sim 100\%$  in both cultures. The MTT assay applied directly to the microfibers further

confirmed high cell viability and metabolic activity (Fig. 2).

Although the cells stayed viable and metabolically active in both cultures (Fig. 2), cell proliferation was enhanced only under continuous medium flow, which in this case induced positive effects on the cells. It should be noted that the direct comparison of these results with Experiment 1 is not possible due to differences in the cell type, hydrogel form, and medium flow rate. However, a comparison of the results obtained in the static and bioreactor cultures in Experiment 2 implies that the static culture was mass transfer limited regarding some nutrient or bioactive molecule. Therefore, two hypotheses for limiting substances were tested, namely: i) oxygen, as usually considered, a rate-limiting factor for the proliferation of cancer cells (*e.g.*, [48,49]), and ii) a larger bioactive molecule (*e.g.*, proteins, hormones, or growth factors) present in FBS that could trigger the cell proliferation if efficiently supplied (as under perfusion). In the second case, transferrin was selected as a model molecule due to its significant role in the metabolism of cancer cells as a transporter of iron, possibly facilitating cell proliferation [50].

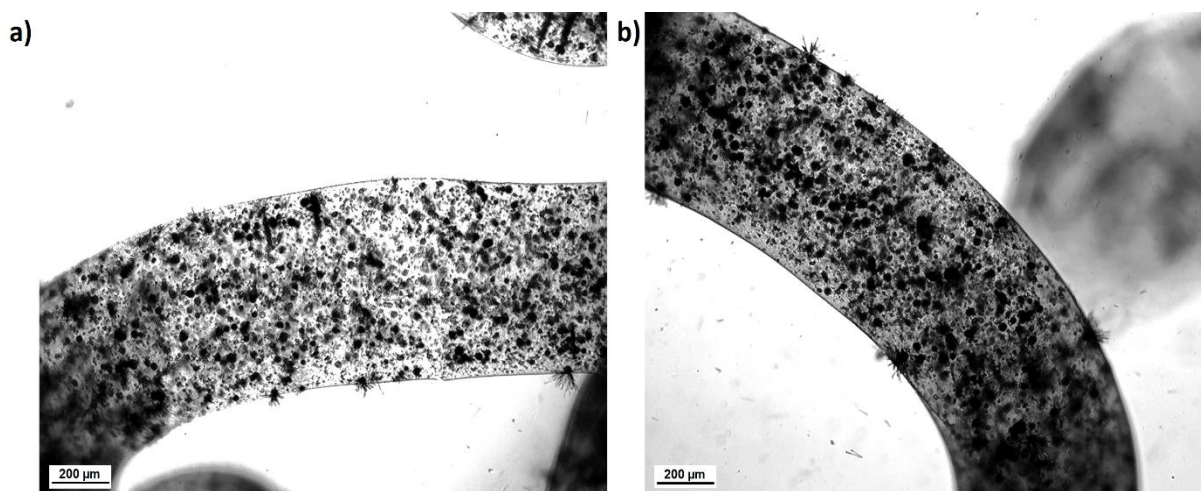


Figure 2. Optical micrographs of MTT-stained microfibers cultivated for 13 days in total: a) under static conditions; b) under static conditions for 8 days followed by 5 days under continuous perfusion (scale bar:  $200$   $\mu\text{m}$ ). Dark dots indicate purple formazan crystals formed by enzymatic reduction of the tetrazolium dye MTT in viable cells.

## Mathematical modeling of mass transport in the fibrous bed bioreactor

### Mass transport without consumption

Mathematical modeling of mass transport in the fibrous bed bioreactor was founded on the assumption that the internal transport through the microfibers is rate-limiting and that the external mass transfer resistance to the microfiber surfaces is negligible. In addition, based on the observation of the effects of the medium flow on NT2/D1 cells within alginate

microbeads in Experiment 1 and the previous modeling studies of the silver release from the nanocomposite Ag/alginate microbeads [44], it was assumed that a small fraction of the medium flow is passing through the microfibers, thus increasing the internal mass transport rate compared to diffusion only, present in the static culture. Therefore, the experiments were performed with Ag/honey/alginate microfibers to determine silver

release mechanisms and the interstitial flow through the microfibers under continuous perfusion. The same approach was conducted in the previous silver release study from the packed bed of Ag/alginate microbeads [44]. In brief, the produced Ag/honey/alginate microfibers using two batches of honey had statistically similar diameters (average  $670 \pm 140 \mu\text{m}$ ) and silver concentrations (average  $2.9 \pm 0.4 \text{ mM}$ ) as determined by AAS. At the same time, the presence of AgNPs was confirmed by UV-vis spectroscopy (Fig. 1S, Supplementary material). Furthermore, over 7 days under perfusion at the superficial velocity of  $80 \mu\text{m s}^{-1}$ , silver release deviated from Fick's law of diffusion and was modeled by a diffusion-advection equation. Specifically, the nanocomposite microfiber bed was modeled as a compact hydrogel cylinder, 3 cm in length (based on experimental measurements of the bed height). It was assumed that the AgNP oxidation is faster than the mass transport of silver species through the hydrogel so that the change of silver concentration,  $c_s$ , in the cylindrical hydrogel over time is described by the diffusion-advection equation in the axial direction,  $x$ :

$$\frac{\partial c_s}{\partial t} = D_s \left( \frac{\partial^2 c_s}{\partial x^2} \right) - u \frac{\partial c_s}{\partial x} \quad (3)$$

where  $D_s$  is the apparent silver diffusion coefficient (of AgNPs,  $\text{Ag}^+$  and formed  $\text{AgCl}_x^{(x-1)-}$  species) in the alginate hydrogel adopted as  $2.1 \times 10^{-15} \text{ m}^2 \text{ s}^{-1}$  [51] and  $u$  is the medium velocity through the hydrogel. Silver concentration in the medium,  $c_{sm}$ , at each time point is calculated then as:

$$c_{sm} = \frac{V(c_{s0} - \langle c_s \rangle)}{V_m} \quad (4)$$

where  $c_{s0}$  is the initial silver concentration in microfibers ( $2.9 \times 10^{-3} \text{ mol dm}^{-3}$  as the average measured concentration),  $\langle c_s \rangle$  is the average silver concentration in the hydrogel,  $V$  is the hydrogel volume (calculated as  $0.49 \text{ cm}^3$  based on the microfiber mass and the alginate density of  $1020 \text{ kg m}^{-3}$  [51]), and  $V_m$  is the medium volume ( $15 \text{ cm}^3$ ). A negligible silver concentration in the medium compared to that in the hydrogel was assumed so that the inlet silver concentration was set to 0. The Neumann boundary condition was set at the outlet boundary. The modeling approach is summarized in the Supplementary material. The numerical solution of the model equations yielded the predictions that agreed well with the experimentally measured silver concentrations in the culture medium (Fig. 3). It should be noted that large error bars at later days of silver release are due to higher AgCl deposition in the system at these times, inducing scattering of experimentally measured data. The medium interstitial velocity through the hydrogel was predicted to be  $10.2 \text{ nm s}^{-1}$ , which agrees with the previously determined value of

$4.6 \text{ nm s}^{-1}$  through Ag/alginate microbeads in a packed bed [44].

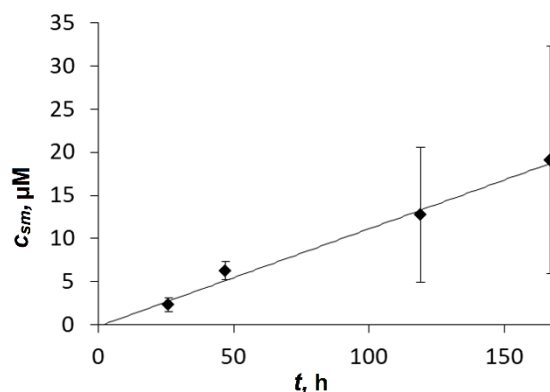


Figure 3. Released silver concentration from Ag/honey/alginate microfibers ( $c_{sm}$ ) as a function of time ( $t$ ) under perfusion: experimental data (symbols) and modeling results (lines) (data represent the average of  $n=3$ ).

#### Mass transport in the cell culture with the consumption term

Based on the obtained modeling results of silver release from packed beds of Ag/honey/alginate microfibers under perfusion, mass transport models were set to describe the transport of active substances within a single microfiber under cell culture conditions. Specifically, a model based on diffusion, advection, and reaction was set up to determine the concentration levels of different substances throughout a single microfiber under perfusion conditions. In contrast, a diffusion-reaction model was formulated to describe mass transport within a microfiber under static conditions. In both cases, the following assumptions were made:

1. the cylindrical geometry of the microfiber;
2. the constant microfiber diameter;
3. the constant consumption rate of the modeled substance per cell (zero-order chemical reaction);
4. the constant concentration of the modeled substance in the medium and thus at the microfiber surface;
5. mass transport only along the radial direction.

Therefore, the mass transport within a microfiber in the bioreactor culture was described by the diffusion-advection-reaction equation:

$$\frac{\partial c}{\partial t} = \frac{D}{r} \frac{\partial}{\partial r} \left( r \frac{\partial c}{\partial r} \right) - u \frac{\partial c}{\partial r} - \rho q \quad (5)$$

where  $D$  is the diffusion coefficient of the modeled substance,  $r$  is the radial coordinate from the microfiber center,  $q$  is the consumption rate of the substance per cell,  $\rho$  is the cell concentration per the microfiber volume, and  $u$  is the interstitial medium velocity within the microfiber in the radial direction.

The same equation describes the mass transport within a microfiber under static conditions with the omitted advective term:

$$\frac{\partial c}{\partial t} = \frac{D}{r} \frac{\partial}{\partial r} \left( r \frac{\partial c}{\partial r} \right) - \rho q \quad (6)$$

#### Initial and boundary conditions

Initial conditions depended on the modeled substance. In the case of oxygen, the initial concentration at time  $t = 0$  is uniform throughout the entire microfiber and is equal to the medium concentration,  $c_m$ :

$$t = 0 \quad 0 \leq r \leq R \quad c = c_m \quad (7)$$

where  $R$  is the microfiber radius. In the case of transferrin or other limiting substance present in the cell medium, the initial concentration in the microfiber is equal to zero that is:

$$t = 0 \quad 0 \leq r \leq R \quad c = 0 \quad (8)$$

The symmetry boundary condition was set along the microfiber axis that is:

$$r = 0 \quad \frac{dc}{dr} = 0 \quad (9)$$

At the outer microfiber boundary, a constant concentration equal to that in the medium ( $c_m$ ) was assumed:

$$r = R \quad c = c_m \quad (10)$$

#### Numerical solution

Partial differential equations (5) and (6) were solved numerically. The second concentration derivative was solved using the centered finite difference method, while for the first concentration derivative, the forward finite difference and backward finite difference methods were used.

#### Model parameters

The microfiber diameter was set to 540  $\mu\text{m}$ , which is the average value of all measured microfiber diameters before and after the static and bioreactor cultures.

The interstitial velocity of the culture medium within the microfiber under perfusion conditions ( $u$ ) was adopted as 10.2  $\text{nm s}^{-1}$  based on the experimental and mathematical modeling studies of silver release from nanocomposite Ag/alginate microfibers. The cell density in microfibers was set to the initial value of  $1.5 \times 10^6 \text{ cells cm}^{-3}$ .

#### Modeling of oxygen transport

The oxygen diffusion coefficient was set to  $D = 1.79 \times 10^{-9} \text{ m}^2 \text{ s}^{-1}$  as reported in the literature for the 3 wt.% alginate hydrogel [52], while a oxygen

concentration in the culture medium was adopted as  $0.18 \text{ mol m}^{-3}$  [53]. The oxygen consumption rate per cell for the C6 rat glioma cell line was reported to be  $12 \times 10^{-18} \text{ mol cell}^{-1} \text{ s}^{-1}$  [54].

Oxygen concentration profiles upon reaching a steady-state in both cultures are plotted as a function of the normalized radial distance concerning the microfiber radius (Fig. 4).

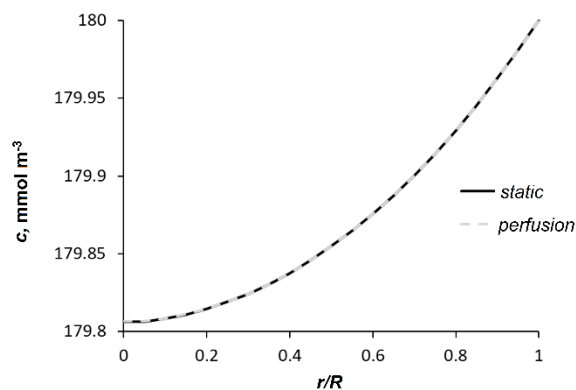


Figure 4. Oxygen concentration ( $c$ ) profiles as functions of the normalized radial distance within a microfiber ( $r/R$ ) upon reaching the steady-state under static and continuous perfusion conditions at the initial cell density of  $1.5 \times 10^6 \text{ cells cm}^{-3}$  ( $R$  is the microfiber radius;  $r/R=0$  designates the microfiber central axis, while  $r/R=1$  designates the microfiber outer surface).

In both cultures, the steady-state is reached almost immediately (after 73 s and 63 s in the static and bioreactor cultures, respectively) with the oxygen concentration in the center of the microfiber of 99.9% with respect to that in the culture medium. Thus, the modeling results imply efficient mass transport under both culture conditions, with diffusion being sufficient to fulfill the oxygen needs of the cells immobilized in alginate microfibers at the investigated density without any hypoxic regions. We have further modeled oxygen diffusion within microfibers with the final experimental cell density of  $8.8 \times 10^6 \text{ cells cm}^{-3}$  reached in the bioreactor culture only, and still transport by diffusion would be sufficient without visible effects of additional advective transport. In this case, the steady-state would be reached after 82 s in static and 78 s in bioreactor cultures, with the oxygen concentration in the microfiber center of 99.4% with regard to that in the medium in both cultures.

Thus, it could be assumed that static conditions could efficiently support the supply of gases and small molecules with diffusion coefficients of  $\sim 10^{-9} \text{ m}^2 \text{ s}^{-1}$  to the cells immobilized in alginate microfibers at the investigated cell density range up to  $\sim 9 \times 10^6 \text{ cells cm}^{-3}$ . Furthermore, the effects of advective mass transport, in this case, are negligible. Hence, the reason for

increased cell proliferation under medium flow conditions could be sought in the transport of a larger molecule.

### Modeling of transferrin transport

FBS is a complex natural product containing many various nutritional and bioactive components, including numerous types of proteins. Albumin is the most abundant protein in bovine serum, comprising 60–67% of total proteins, while transferrin is found at a fairly constant concentration ranging from 1.37 to 3.72 mg cm<sup>-3</sup> [55]. Transferrin was reported to play a significant role in the metabolism of cancer cells [50]. Moreover, the transferrin receptor 1 was found to participate in the regulation of glioma cell physiology, where the resulting iron accumulation and reactive oxygen species (ROS) formation facilitate the proliferation of these cells [50]. Therefore, we have assumed that the mass transport of transferrin may be an important parameter in 3D glioma cell cultures.

Transferrin serves as a transporter of iron to cells and, after internalization, is exocytosed back to the medium. The overall consumption rate of transferrin per cell was reported to be 2.6×10<sup>-22</sup> mol cell<sup>-1</sup> s<sup>-1</sup> [56]. Furthermore, the diffusion coefficient of transferrin in agarose gels was reported as 5.3×10<sup>-11</sup> m<sup>2</sup> s<sup>-1</sup> [57]. Finally, taking into account an average transferrin concentration in FBS of 2.5 mg cm<sup>-3</sup> diluted 10-fold in the culture medium, the transferrin medium concentration was adopted for modeling purposes as  $c_m = 3.1 \times 10^{-3}$  mol m<sup>-3</sup>.

Numerical solution of Eqs. (5) and (6) yielded the steady-state in static and bioreactor cultures after 36.2 and 35.7 min, respectively, reaching the transferrin concentration in the microfiber center of 99.98% with respect to that in the culture medium. Figure 5 shows transferrin concentration profiles in microfibers after 10 min in both cultures to illustrate slight differences in the transport rates before reaching the steady-state.

Based on the obtained results, it can be concluded that similarly as in the case of oxygen, the static conditions provide efficient transport of transferrin. Thus, the impact of advection on mass transport rates is negligible. Still, it should be noted that the transferrin molecule could interact with COO-groups [58], which are also present in alginate polymer chains. Therefore, these groups may be hindering the transferrin diffusion through the alginate hydrogel yielding a lower diffusion coefficient than the value used for mathematical modeling in this study. Moreover, alginate was used in a study of the controlled release of lactoferrin [59], a molecule with a similar sequence and

structure as transferrin, and coordinates iron identically [60]. In specific, when lactoferrin was adsorbed onto calcium phosphate nanoparticles further covered with chitosan and alginate layers, the *in vitro* release in PBS lasted over 10 h [59], implying a significantly lower release rate with the apparent diffusion coefficient of about 10<sup>-19</sup>–10<sup>-20</sup> m<sup>2</sup> s<sup>-1</sup>.

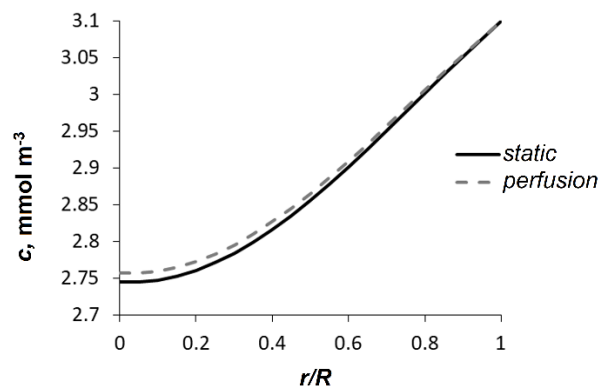


Figure 5. Predicted transferrin concentration ( $c$ ) profiles as functions of the normalized radial distance within a microfiber ( $r/R$ ) after 10 min under static and continuous perfusion conditions ( $R$  is the microfiber radius;  $r/R=0$  designates the microfiber central axis, while  $r/R=1$  designates the microfiber outer surface).

Therefore, we have checked the effects of a decreased diffusion coefficient in the investigated cultures in the next step. Figure 6 shows the modeling results of transferrin transport with the diffusion coefficient of  $D = 1 \times 10^{-19}$  m<sup>2</sup> s<sup>-1</sup>. In this case, advection is the dominant mass transport mechanism in the bioreactor culture. The transferrin concentration within the alginate microfiber in static cultures stayed approximately constant over 5 days due to the approximately equal diffusion and consumption rates (Fig. 6b). On the contrary, the transferrin concentrations in the microfiber in the bioreactor culture almost reached that existing in the medium after 7 h (Fig 6a). The obtained results suggest that the transferrin supply in static cultures may have been insufficient, leading to slow proliferation. In contrast, the advective transport compensated for slow diffusion in the bioreactor cultures. However, it is also possible that the transferrin apparent diffusion coefficient is between the values used in the present study and that a different substance with similar transport properties influenced the cell proliferation in our experiment. The modeling results indicate that substances with lower diffusion coefficients ( $D \sim 10^{-19}$  m<sup>2</sup> s<sup>-1</sup>) are transported very slowly under static conditions so that the convective mass transfer is necessary for efficient delivery.

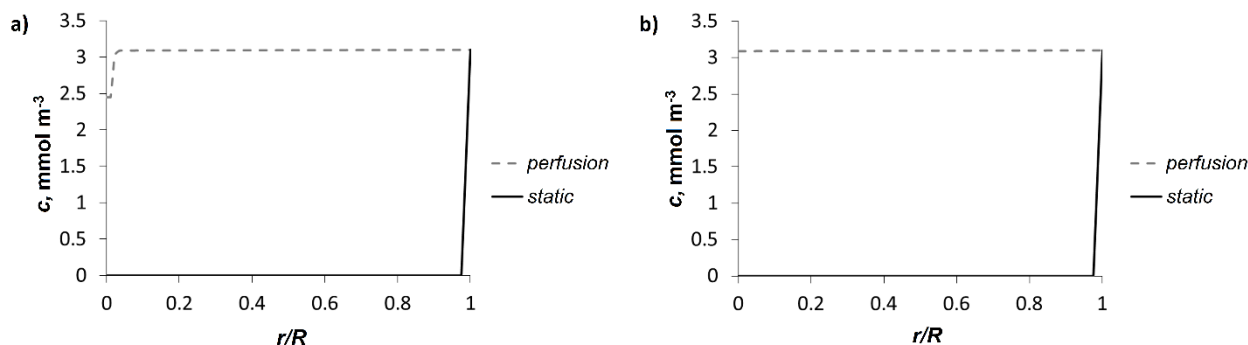


Figure 6. Predicted transferrin concentration ( $c$ ) profiles with a decreased diffusion coefficient of  $D = 1 \times 10^{-19} \text{ m}^2 \text{ s}^{-1}$  as functions of the normalized radial distance within a microfiber ( $r/R$ ) under static and continuous perfusion conditions: a) after 7 hours; b) after 5 days of cultivation ( $R$  is the microfiber radius;  $r/R=0$  designates the microfiber central axis, while  $r/R=1$  designates the microfiber outer surface).

## CONCLUSION

In this work, two independent 3D cultures of different cancer cells were preliminary experimentally investigated while chemical engineering methods were used to analyze and interpret the obtained results. In Experiment 1, continuous superficial velocity of  $80 \mu\text{m s}^{-1}$  was indicated as unfavorable for survival of cancer cells NT2/D1 in alginate microbead superficial zones. Application of the Carman-Kozeny equation yielded the shear stress of 67 mPa, equal to the upper reported physiological level. In Experiment 2, the superficial velocity of  $100 \mu\text{m s}^{-1}$  enhanced the proliferation of glioma cancer cells C6 immobilized in alginate microfibers compared to the static control culture. A simple mass transport model within microfibers indicated that the substances with diffusivities of  $\sim 10^{-9}$ - $10^{-11} \text{ m}^2 \text{ s}^{-1}$  are sufficiently supplied by diffusion only. In contrast, for the substances with significantly lower diffusivities ( $\sim 10^{-19} \text{ m}^2 \text{ s}^{-1}$ ), convective transport is necessary for the efficient provision to the immobilized cells. Although the results of Experiments 1 and 2 could not be directly compared, applying chemical engineering methods provided an estimation of certain culture parameters (*i.e.*, hydrodynamic shear stress level and mass transport mechanisms and rates) that could have induced the observed results indicating future directions for the culture system optimization.

## Acknowledgment

This work was supported by funding from the European Union's Horizon 2020 research and innovation program under grant agreement no. 952033 and by the Ministry of Education, Science and Technological Development RS (Contracts No. 451-03-9/2021-14/200135, 451-03-9/2021-14/200287, and 451-03-9/2021-14/200042). We thank Prof. Peter W. Andrews (University of Sheffield, UK) for NT2/D1 cells.

## REFERENCES

- [1] H. Sung, J. Ferlay, R.L. Siegel, M. Laversanne, I. Soerjomataram, A. Jemal, F. Bray, *Ca-Cancer J. Clin.* 71 (2021) 209-249.
- [2] M. Kapalczyńska, T. Kolenda, W. Przybyła, M. Zajączkowska, A. Teresiak, V. Filas, M. Ibbs, R. Bliźniak, Ł. Łuczewski, K. Lamperska, *Arch. Med. Sci.* 14 (2018) 910-919.
- [3] H. Ungefroren, S. Sebens, D. Seidl, H. Lehnert, R. Hass, *Cell Commun. Signaling* 9 (2011) 1-8.
- [4] J.A. Hickman, R. Graeser, R. de Hoogt, S. Vidic, C. Brito, M. Gutekunst, H. van der Kuip, *Biotechnol. J.* 9 (2014) 1115-1128.
- [5] A. Nyga, U. Cheema, M. Loizidou, *J. Cell Commun. Signaling* 5 (2011) 239-248.
- [6] M.D. Szeto, G. Chakraborty, J. Hadley, R. Rockne, M. Muzi, E.C. Alvord, K.A. Krohn, A.M. Spence, K.R. Swanson, *Cancer Res.* 69 (2009) 4502-4509.
- [7] N. Filipovic, T. Djukic, I. Saveljic, P. Milenkovic, G. Jovicic, M. Djuric, *Comput. Methods Programs Biomed.* 115 (2014) 162-170.
- [8] P. Caccavale, M.V. De Bonis, G. Marino, G. Ruocco, *Int. Commun. Heat Mass Transfer* 117 (2020) 104781.
- [9] T. Chen, N.F. Kirkby, R. Jena, *Comput. Methods Programs Biomed.* 108 (2012) 973-983.
- [10] D. Karami, N. Richbourg, V. Sikavitsas, *Cancer Lett. (N. Y., NY, U. S.)* 449 (2019) 178-185.
- [11] D. Massai, G. Isu, D. Madeddu, G. Cerino, A. Falco, C. Frati, D. Gallo, M.A. Deriu, G. Falvo D'Urso Labate, F. Quaini, A. Audenino, U. Morbiducci, *PloS One* 11 (2016) e0154610.
- [12] J.E. Trachtenberg, M. Santoro, C. Williams III, C.M. Piard, B.T. Smith, J.K. Placone, B.A. Menegaz, E.R. Molina, S.-E. Lamhamedi-Cherradi, J.A. Ludwig, V.I. Sikavitsas, J.P. Fisher, A.G. Mikos, *ACS Biomater. Sci. Eng.* 4 (2018) 347-356.
- [13] C.M. Novak, E.N. Horst, C.C. Taylor, C.Z. Liu, G. Mehta, *Biotechnol. Bioeng.* 116 (2019) 3084-3097.
- [14] V.S. Shirure, S.F. Lam, B. Shergill, Y.E. Chu, N.R. Ng, S.C. George, *Lab Chip* 20 (2020) 3036-3050.
- [15] K.Y. Lee, D.J. Mooney, *Prog. Polym. Sci.* 37 (2012) 106-126.
- [16] K.I. Draget, G. Skjåk-Bræk, O. Smidsrød, *Int. J. Biol. Macromol.* 21 (1997) 47-55.
- [17] P. Sánchez, R.M. Hernández, J.L. Pedraz, G. Orive, in

- Immobilization of Enzymes and Cells, Humana Press, Totowa, NJ (2013) 313-325.
- [18] B.R. Lee, K.H. Lee, E. Kang, D.S. Kim, S.H. Lee, *Biomicrofluidics* 5 (2011) 022208.
- [19] F.M. Kievit, S.J. Florczyk, M.C. Leung, O. Veiseh, J.O. Park, M.L. Disis, M. Zhang, *Biomaterials* 31 (2010) 5903-5910.
- [20] M. Leung, F.M. Kievit, S.J. Florczyk, O. Veiseh, J. Wu, J.O. Park, M. Zhang, *Pharm. Res.* 27 (2010) 1939-1948.
- [21] S.J. Florczyk, G. Liu, F.M. Kievit, A.M. Lewis, J.D. Wu, M. Zhang, *Adv. Healthcare Mater.* 1 (2012) 590-599.
- [22] Q. Wang, S. Li, Y. Xie, W. Yu, Y. Xiong, X. Ma, Q. Yuan, *Hepato. Res.* 35 (2006) 96-103.
- [23] M.L. Tang, X.J. Bai, Y. Li, X.J. Dai, F. Yang, *Curr. Med. Sci.* 38 (2018) 809-817.
- [24] C. Liu, D.L. Mejia, B. Chiang, K.E. Luker, G.D. Luker, *Acta Biomater.* 75 (2018) 213-225.
- [25] N. Chaicharoenaudomrung, P. Kunhorm, W. Promjantuek, N. Heebkaew, N. Rujanapun, P. Noisa, *J. Cell. Physiol.* 234 (2019) 20085-20097.
- [26] K. Xu, K. Ganapathy, T. Andl, Z. Wang, J.A. Copland, R. Chakrabarti, S.J. Florczyk, *Biomaterials* 217 (2019) 119311.
- [27] L.E. Marshall, K.F. Goliwas, L.M. Miller, A.D. Penman, A.R. Frost, J.L. Berry, *J. Tissue Eng. Regener. Med.* 11 (2017) 1242-1250.
- [28] M. Santoro, S.E. Lamhamedi-Cherradi, B.A. Menegaz, J.A. Ludwig, A.G. Mikos, *Proc. Natl. Acad. Sci. U. S. A.* 112 (2015) 10304-10309.
- [29] X. Wan, Z. Li, H. Ye, Z. Cui, *Biotechnol. Lett.* 38 (2016) 1389-1395.
- [30] M.G. Muraro, S. Muenst, V. Mele, L. Quagliata, G. Iezzi, A. Tzankov, W.P. Weber, G.C. Spagnoli, S.D. Soysal, *Oncolimmunology* 6 (2017) e1331798.
- [31] X. Wan, S. Ball, F. Willenbrock, S. Yeh, N. Vlahov, D. Koennig, M. Green, G. Brown, S. Jeyaretna, Z. Li, Z. Cui, H. Ye, E. O'Neill, *Sci. Rep.* 7 (2017) 1-13.
- [32] C. Manfredonia, M.G. Muraro, C. Hirt, V. Mele, V. Governa, A. Papadimitropoulos, S. Däster, S.D. Soysal, R.A. Drosner, R. Mechera, D. Oertli, R. Rosso, M. Bolli, A. Zettl, L.M. Terracciano, G.C. Spagnoli, I. Martin, G. Iezzi, *Adv. Biosyst.* 3 (2019) 1800300.
- [33] C. Hirt, A. Papadimitropoulos, M.G. Muraro, V. Mele, E. Panopoulos, E. Cremonesi, R. Ivanek, E. Schultz-Thater, R. Drosner, C. Mengus, M. Hebeber, D. Oertli, G. Iezzi, P. Zajac, S. Eppenberger-Castori, L. Tornillo, L. Terracciano, I. Martin, G.C. Spagnoli, *Biomaterials* 62 (2015) 138-146.
- [34] F. Foglietta, G.C. Spagnoli, M.G. Muraro, M. Ballestri, A. Guerrini, C. Ferroni, A. Aluigi, G. Sotgiu, G. Varchi, *Int. J. Nanomed.* 13 (2018) 4847-4867.
- [35] H. Qazi, Z.-D. Shi, J.M. Tarbell, *PLoS One* 6 (2011) e20348.
- [36] D.H. Tryoso, D.A. Good, *J. Physiol.* 515.2 (1999) 355-365.
- [37] L. Ziko, S. Riad, M. Amer, R. Zdero, H. Bougherara, A. Amleh, *Biomed. Res. Int.* 2015 (2015), ID 430569.
- [38] A. Marrella, A. Fedi, G. Varani, I. Vaccari, M. Fato, G. Firpo, P. Guida, N. Aceto, S. Scaglione, *PLoS One* 16 (2021) e0245536.
- [39] J. Stojkowska, B. Bugarski, B. Obradovic, *J. Mater. Sci.: Mater. Med.* 21 (2010) 2869-2879.
- [40] A. Osmokrovic, B. Obradovic, D. Bugarski, B. Bugarski, G. Vunjak-Novakovic, *FME Trans.* 34 (2006) 65-70.
- [41] J. Stojkowska, J. Zvicer, M. Milivojević, I. Petrović, M. Stevanović, B. Obradović, *Hem. Ind.* 74 (2020) 187-196.
- [42] J. Stojkowska, P. Petrovic, I. Jancic, M.T. Milenkovic, B. Obradovic, *Appl. Microbiol. Biotechnol.* 103 (2019) 8529-8543.
- [43] J. Stojkowska, J. Zvicer, Ž. Jovanović, V. Mišković-Stanković, B. Obradović, *J. Serb. Chem. Soc.* 77 (2012) 1709-1722.
- [44] D.D. Kostic, I.S. Malagurski, B.M. Obradovic, *Hem. Ind.* 71 (2017) 383-394.
- [45] R.G. Holdich, *Fundamentals of particle technology*, Midland Information Technology and Publishing, Hathern, Leicestershire (2002) 45-54.
- [46] E. Fröhlich, G. Bonstingl, A. Höfler, C. Meindl, G. Leitinger, T.R. Pieber, E. Roblegg, *Toxicol. In Vitro* 27 (2013) 409-417.
- [47] M.J. Mitchell, M.R. King, *Front. Oncol.* 3 (2013) 44.
- [48] Y. Chen, R. Cairns, I. Papandreou, A. Koong, N.C. Denko, *PLoS One* 4 (2009) e7033.
- [49] A. Gomes, L. Guillaume, D.R. Grimes, J. Fehrenbach, V. Lobjois, B. Ducommun, *PLoS One* 11 (2016) e0161239.
- [50] Y. Shen, X. Li, D. Dong, B. Zhang, Y. Xue, P. Shang, *Am. J. Cancer Res.* 8 (2018) 916-931.
- [51] D. Kostic, S. Vidovic, B. Obradovic, *J. Nanopart. Res.* 18 (2016) 76-92.
- [52] A.C. Hulst, H.J.H. Hens, R.M. Buitelaar, J. Tramper, *Biotechnol. Tech.* 3 (1989) 199-204.
- [53] T.L. Place, F.E. Domann, A.J. Case, *Free Radical Biol. Med.* 113 (2017) 311-322.
- [54] B.A. Wagner, S. Venkataraman, G.R. Buettner, *Free Radical Biol. Med.* 51 (2011) 700-712.
- [55] X. Hong, Y. Meng, S.N. Kalkanis, *J. Biol. Methods* 3 (2016) e51.
- [56] A. Ciechanover, A.L. Schwartz, A. Dautry-Varsat, H.F. Lodish, *J. Biol. Chem.* 258 (1983) 9681-9689.
- [57] R. Zadro, B. Pokrić, Z. Pučar, *Anal. Biochem.* 117 (1981) 238-244.
- [58] P. Aisen, I. Listowsky, *Annu. Rev. Biochem.* 49 (1980) 357-393.
- [59] J.R. Kanwar, G. Mahidhara, R.K. Kanwar, *Nanomedicine* 7 (2012) 1521-1550.
- [60] J. Wally, S.K. Buchanan, *BioMetals* 20 (2007) 249-262.

MIA RADONJIĆ <sup>1,2,\*</sup>  
JELENA PETROVIĆ <sup>1,2,\*</sup>  
MILENA MILIVOJEVIĆ <sup>3</sup>  
MILENA STEVANOVIĆ <sup>3,4,5</sup>  
JASMINA STOJKOVSKA <sup>1,2</sup>  
BOJANA OBRADOVIĆ <sup>1</sup>

<sup>1</sup> Univerzitet u Beogradu,  
Tehnološko-metalurški fakultet,  
Beograd, Srbija

<sup>2</sup> Inovacioni centar Tehnološko-  
metalurškog fakulteta, Beograd,  
Srbija

<sup>3</sup> Univerzitet u Beogradu, Institut  
za molekularnu genetiku i  
genetičko inženjerstvo, Beograd,  
Srbija

<sup>4</sup> Univerzitet u Beogradu, Biološki  
fakultet, Beograd, Srbija

<sup>5</sup> Srpska akademija nauka i  
umetnosti, Beograd, Srbija

\* Autori su dali podjednak doprinos radu

NAUČNI RAD

## HEMIJSKO-INŽENJERSKE METODE U ANALIZI 3D KULTURA MALIGNIH ČELIJA: RAZMATRANJE HIDRODINAMIKE I PRENOSA MASE

*U ovom radu, primenjen je multidisciplinarni pristup baziran na eksperimentima i matematičkom modelovanju za razvoj trodimenzionalnih (3D) kultura malignih ćelija. Naime, dve ćelijske linije, ćelije embrionalnog humanog teratokarcinoma NT2/D1 i ćelije glioma pacova C6, imobilisane su u alginatne mikročestice odnosno alginatna mikrovlakna, i gajene u statičkim i u uslovima kontinualnog protoka u protočnim bioreaktorima pri čemu su hemijsko-inženjerski principi primenjeni u analizi dobijenih rezultata. Površinska brzina medijuma za gajenje ćelija od  $80 \mu\text{m s}^{-1}$  je dovela do manje vijabilnosti NT2/D1 ćelija u površinskim zonama mikročestica što je ukazalo na negativne efekte hidrodinamičkih smicajnih napona čija je proračunata vrednost iznosila  $\sim 67 \text{ mPa}$ . Sa druge strane, slična vrednost površinske brzine ( $100 \mu\text{m s}^{-1}$ ) je uticala na povećanje proliferacije C6 glioma ćelija unutar mikrovlakana u odnosu na kontrolu u statičkim uslovima. Dodatna studija otpuštanja srebra iz nanokompozitnih Ag/alginatnih mikrovlakana sa medom u uslovima protoka je pokazala da medijum delimično prolazi kroz sama vlakna (intersticijalnom brzinom od  $\sim 10 \text{ nm s}^{-1}$ ). Prema tome, za opisivanje prenosa mase do imobilisanih ćelija unutar mikrovlakana primenjen je model difuzije sa advекcijom i reakcijom. Pokazano je da je difuzija dovoljan mehanizam prenosa za supstance sa koeficijentima difuzije reda veličine  $\sim 10^9\text{-}10^{11} \text{ m}^2 \text{ s}^{-1}$ , dok je za dopremanje supstanci sa značajno manjim vrednostima koeficijenta difuzije ( $\sim 10^{19} \text{ m}^2 \text{ s}^{-1}$ ) potreban dodatni advекtivni transport. Ovaj rad ilustruje način izbora i doprinos hemijsko-inženjerskih metoda u razvoju in vitro modela tumora.*

*Ključne reči: inženjerstvo tumora, alginatni hidrogel, protočni bioreaktor, matematičko modelovanje, C6 ćelijska linija glioma, ćelijska linija embrionalnog humanog teratokarcinoma NT2/D1.*